Supplementary Information

Hydrogen-bond Engineering Induced Ferroelastic Phase Transition in Copper-based Organic-Inorganic Hybrid Thermochromic Materials

Xin Deng[a], Lin Zhou[a], Xin Yan[a], Yan-Juan Wang[a], Wen-Li Yang[a], Hui-Peng Lv*[a] and Yuan-Yuan Tang*[a]

[a] Ordered Matter Science Research Center, Nanchang University, Nanchang 330031, People's Republic of China.

** Corresponding Authors: tangyuanyuan@ncu.edu.cn, huipenglv@ncu.edu.cn.*

Materials

2-amino-4-methylpyridine, 2-amino-5-methylpyridine, $CuCl_2$ and 36.5% aqueous HCl were commercially available and without further purification.

Synthesis

Synthesis of substance **1,** 10 mmol (1.081 g) 2-amino-5-methylpyridine was dissolved in deionized water and protonated by dropping an appropriate amount of hydrochloric acid aqueous solution. Then, it was mixed with an aqueous solution containing 5 mmol (0.672 g) copper chloride and stirred until the mixed solution was clarified. After the solution was left at undisturbed room temperature for about a week, orange block crystals were obtained.

Synthesis of substance **2**, 10 mmol (1.081 g) 2-amino-4-methylpyridine was dissolved in deionized water and protonated by dropping an appropriate amount of hydrochloric acid aqueous solution. Then, it was mixed with an aqueous solution containing 5 mmol (0.672 g) copper chloride and stirred until the mixed solution was clarified. After the solution was left at undisturbed room temperature for about a week, green sheet-like crystals were obtained.

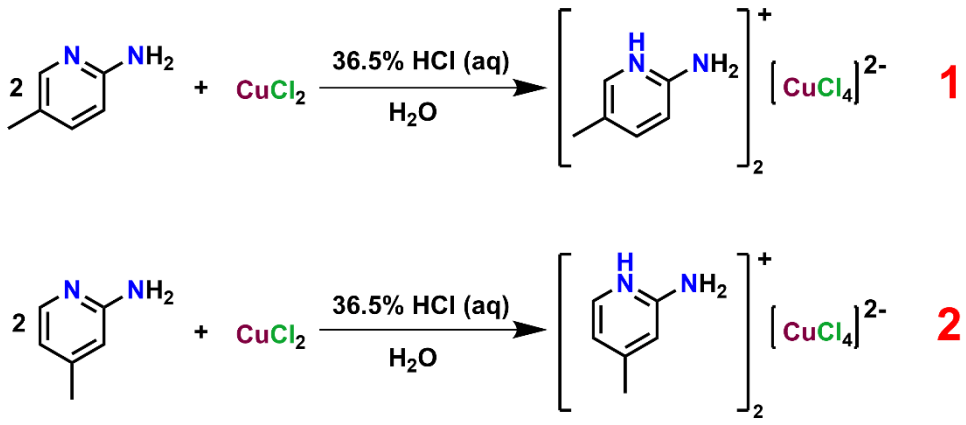

Scheme S1. General synthesis procedure of **1** and **2**.

Methods

Variable-temperature powder X-ray diffraction (PXRD). PXRD measurements were performed on a Rigaku D/MAX 2000 PC X-ray diffractometer in the 2θ range of 5-50˚ with a step size of 0.02˚.

Singe-crystal structure determination. Single-crystal X-ray diffraction data at different temperatures were measured using a Rigaku Saturn 924 diffractometer with Mo-Kα radiation (λ = 0.71073 Å). Data collection and structural refine were performed using Rigaku CrystalClear and SHELXTL software package. The crystal data and structure refinement are summarized in Tables S1-S3 and S6.

Thermal analyses measurements. Differential scanning calorimetry (DSC) measurements were performed using a NETZSCH DSC 200F3 instrument. The powder sample of 4.5 mg was placed in aluminum crucibles and measured under a nitrogen atmosphere at heating and cooling rates of 5 K·min^{-1}, 10 K·min^{-1} and 20 K·min^{-1}. Thermogravimetric analyses (TGA) were carried out on a PerkinElmer TGA 8000 instrument by heating crystalline samples with a rate of 30 K·min^{-1} under a nitrogen atmosphere.

Dielectric measurements. The temperature-dependent dielectric constant was measured using the Tonghui TH2828 analyzer. The method is as follows: The sample sheet with a thickness of approximately 0.5 mm was prepared by pressing the powder polycrystalline sample using a tableting machine. The silver glue was uniformly coated on both sides of the sample sheet, then the copper wires were stuck on it and connected to the six-hole socket to form a capacitor.

Ferroelastic measurements. Prepare a thin film of the compound **2**, and dissolve 5 mg of the crystal powder of **2** in 200 μL dilute hydrochloric acid. Then, 20 μL of solution was added dropwise and evenly spread on a clean indium tin oxide (ITO) glass substrate and PET material plastic, which was placed on a 40 ℃ hot bench. The film of **2** was obtained after annealing at 423 K for about 20 minutes. The stress application comes from manually pressing the PET.

Variable temperature solid state UV-vis absorption. Solid state UV/Vis absorption spectra were recorded by using Shimadzu UV-2600 at temperatures from 293 K to 438 K for **1**, and at temperatures from 299 K to 408 K for **2**.

Hirshfeld surfaces analysis. Hirshfeld surfaces and the related 2D fingerprint plots were calculated by using the CrystalExplorer program with inputting structure files in CIF format.

Nanoindentation characterizations. Nanoindentation tests were performed on a Hysitron TI Premier nanoindenter and dents were imposed by a Berkovich probe. Crystal samples with smooth and flat surface were adhered to a steel SPM puck with cyanoacrylate-based glue, which was then fixed on the instrument stage by magnetostatic force. Standard basic quasi-static trapezoid load function was adopted with a peak load of 1000 μN and loading, holding, and unloading time of 10 s, 0 s, and 10 s, respectively. The indentation curves were acquired from different sites to minimize accidental errors. Values of elastic modulus and hardness were obtained via fitting indentation curves based on the Oliver-Pharr method via packaged software on the instrument.

Infrared-absorption Spectroscopy. Infrared (IR) spectrum was launched on Bruker Invenio R Fouriertransform infrared spectrometers using the sample pelleted with KBr in the region of 4000-400 cm^{-1}. As shown in Figure S9, the infrared characteristic peak positions of **1** and **2** are basically the same.

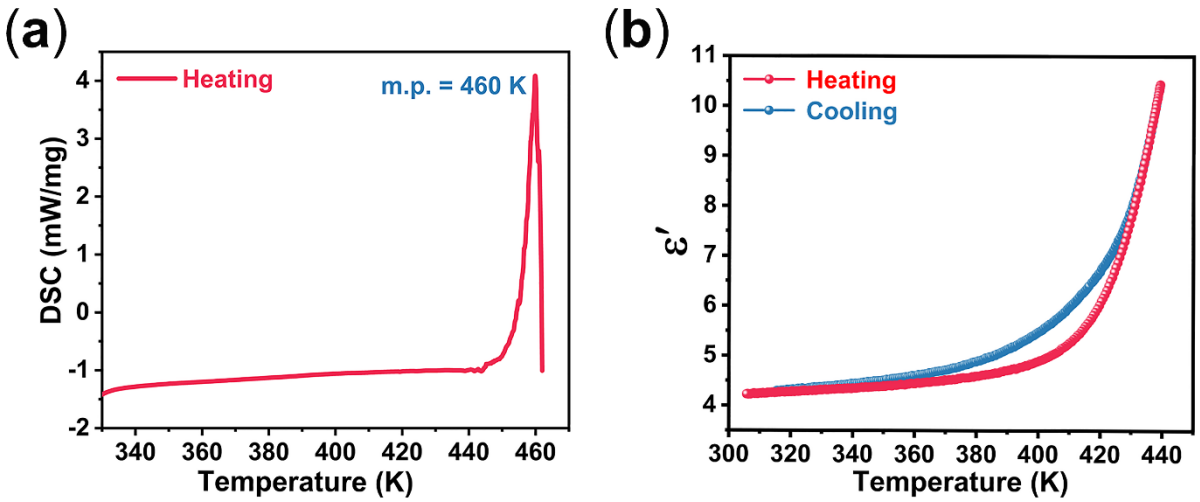

Figure S1. (a) DSC curves of **1** with a scanning rate of 20 K·min^{-1}. (b) Temperature-dependent ε' at 1 MHz upon heating and cooling for **1**.

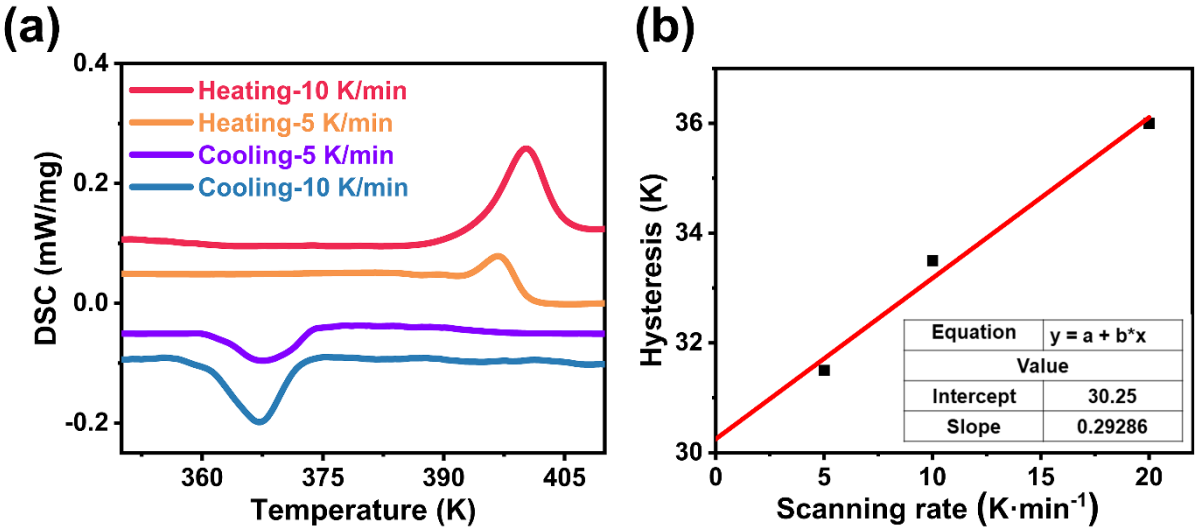

Figure S2. (a) DSC curves of **2** with scanning rates of 5 K·min^{-1} and 10 K·min^{-1}. (b) The limiting thermal hysteresis (30.25 K) estimated from the scans extrapolated to a scanning rate of 0 K·min^{-1}.

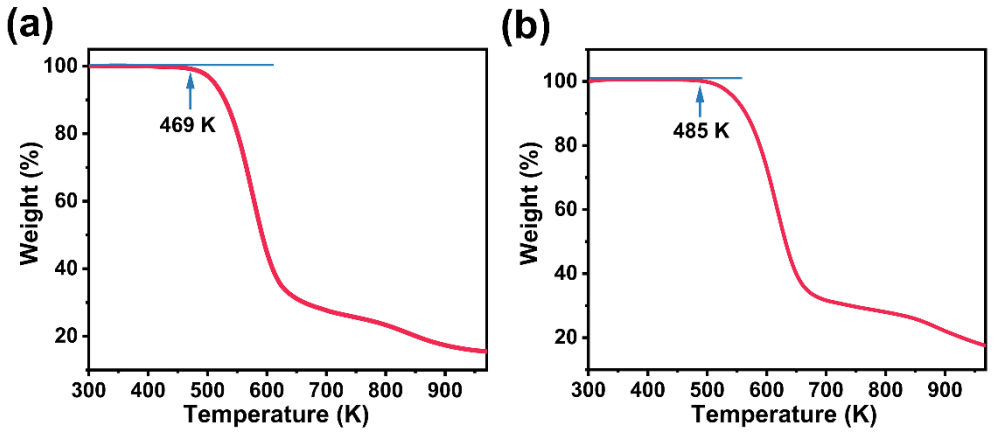

Figure S3. TGA curves of **2** (a) and **1** (b).

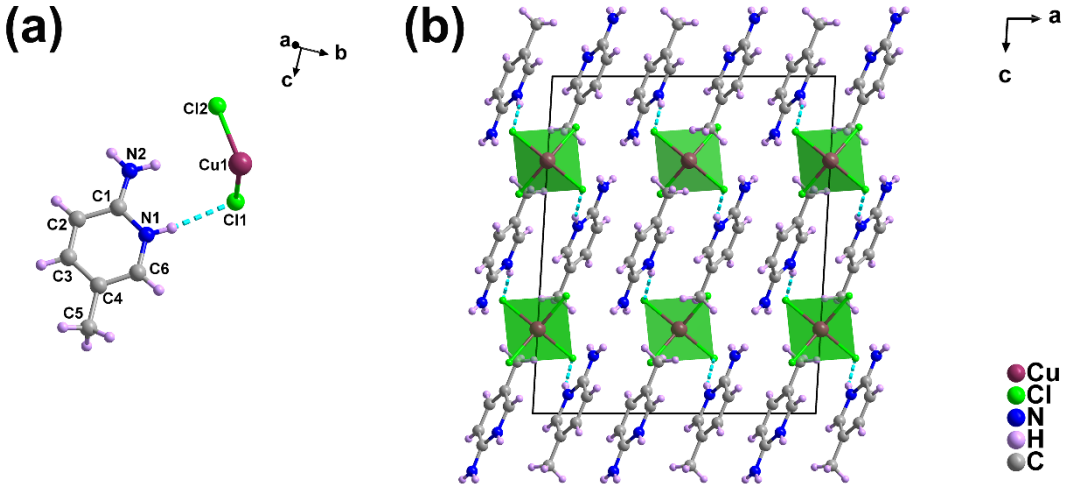

Figure S4. Crystal structure (a) and stacking diagram along the *b*-axis (a) of **1** at 298 K.

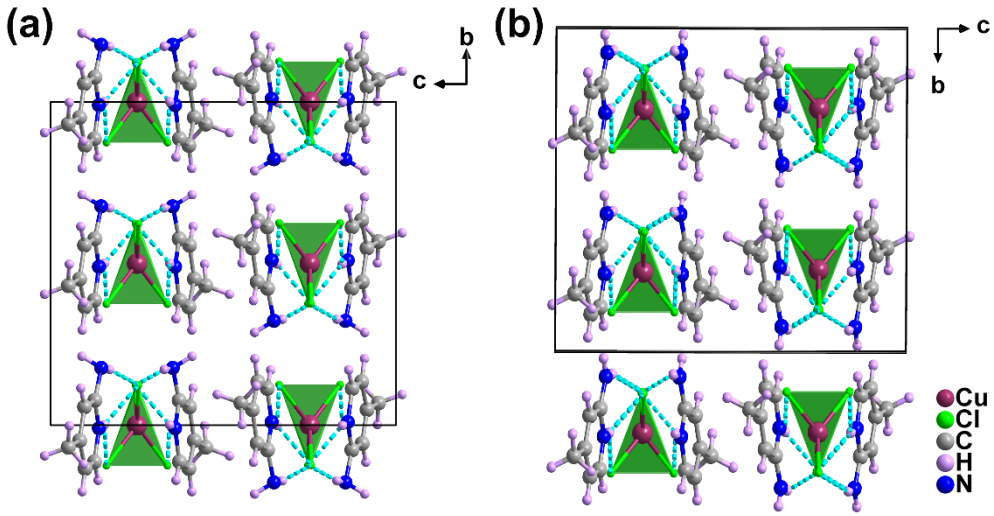

Figure S5. Stacking diagrams along the *a*-axis of **2** at 298 K (a) and 410 K (b).

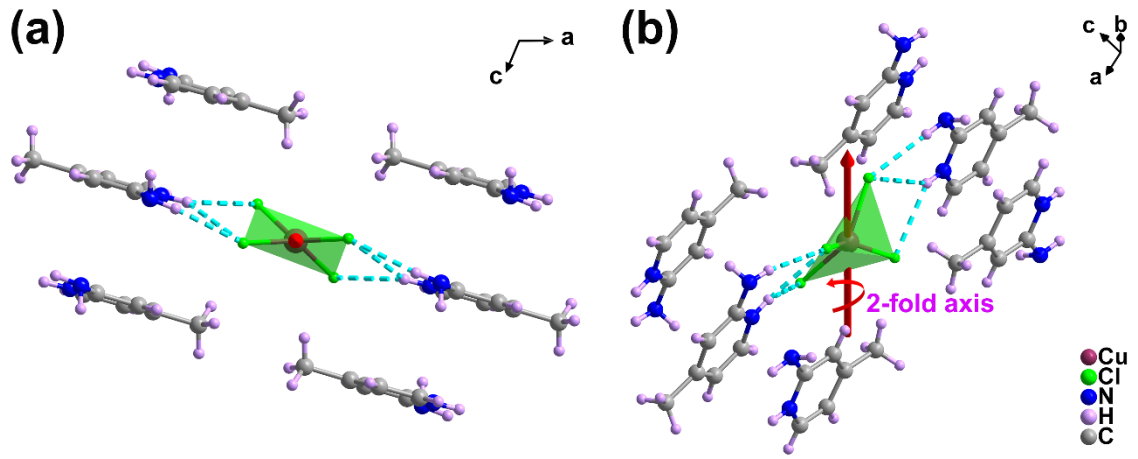

Figure S6. Arrangement diagrams of organic amine cations around the 2-fold axis at 298 K.

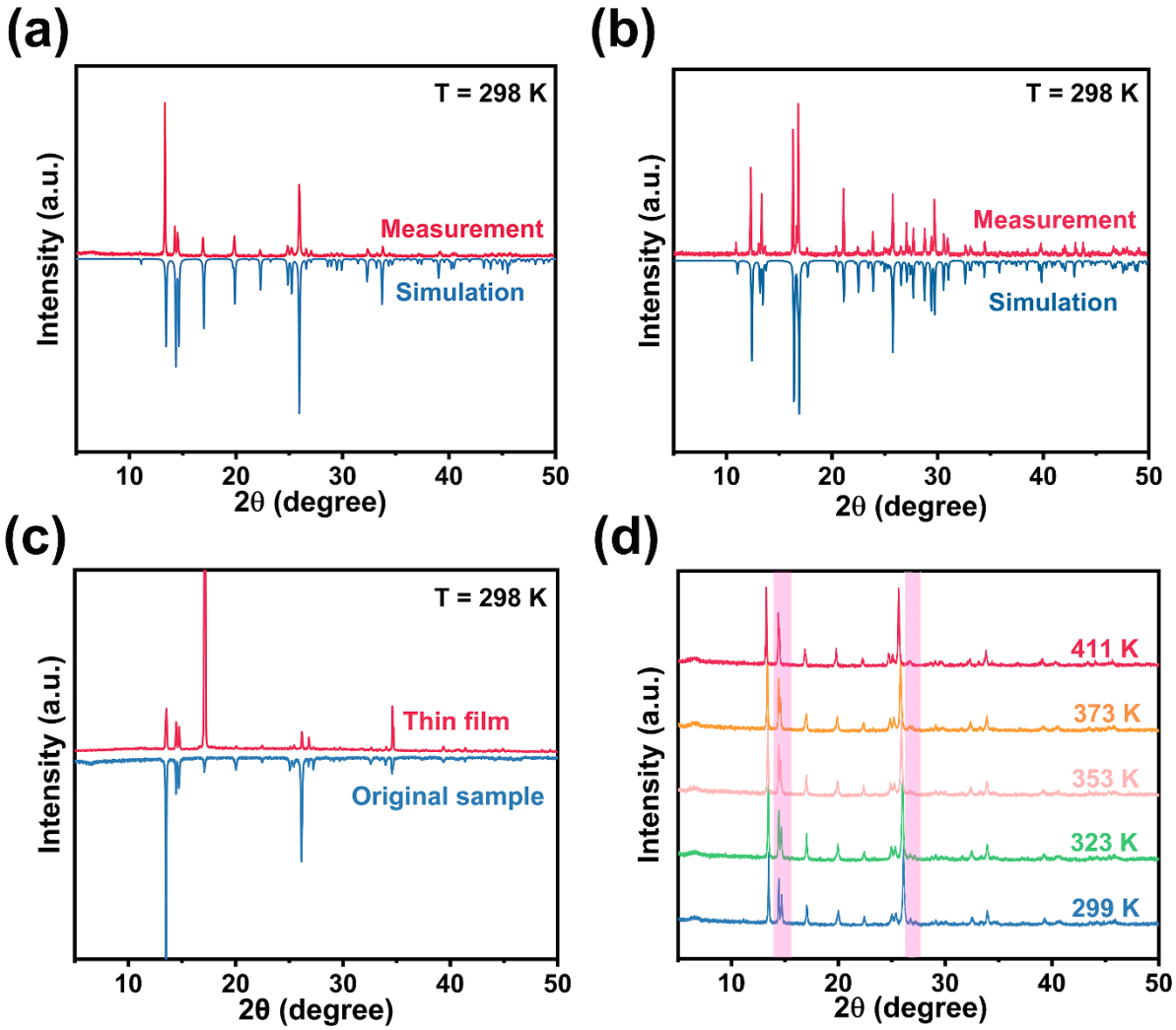

Figure S7. Measured and simulated patterns of the PXRD patterns for **2** (a) and **1** (b) at 298 K. (c) The PXRD patterns of thin films and original samples for **2** at 298 K. (d) The variable-temperature PXRD patterns of **2**.

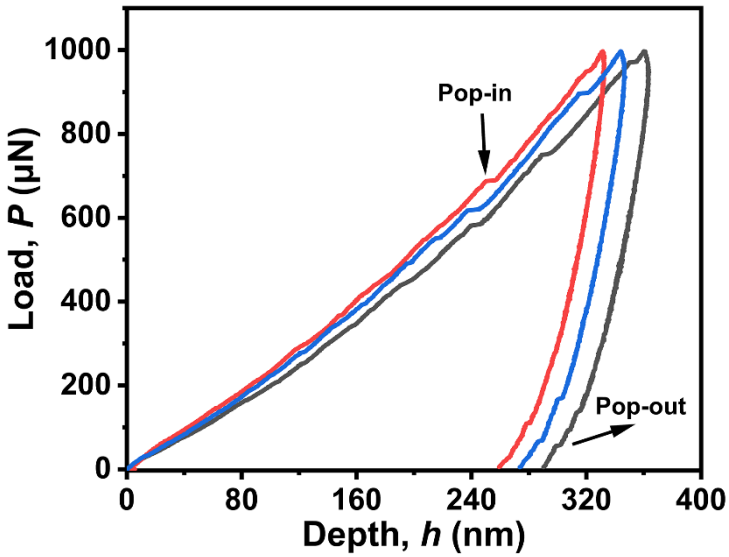

Figure S8. Load-depth curves of **2**.

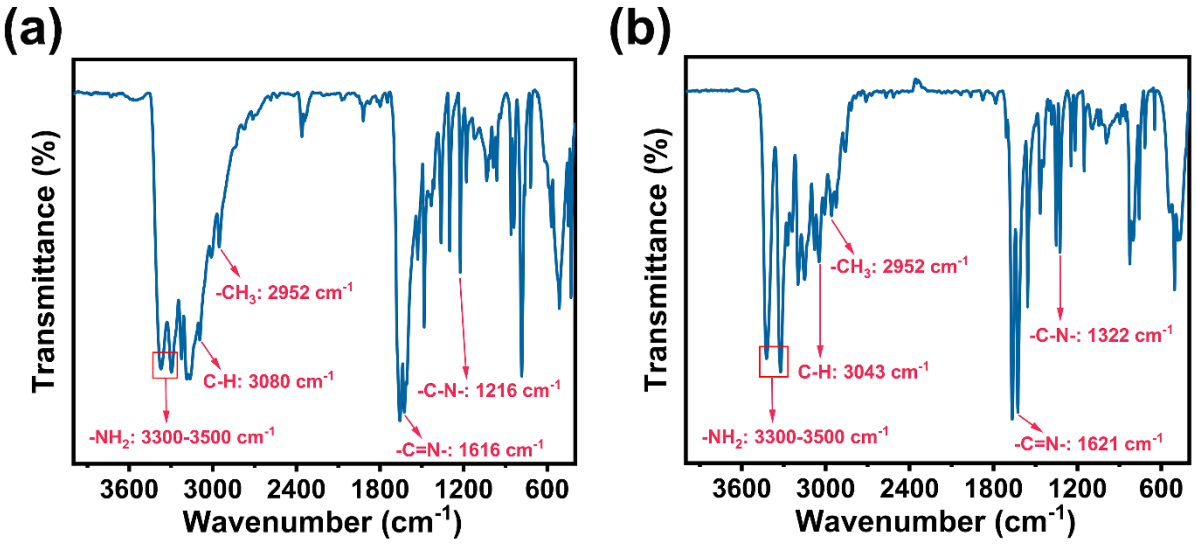

Figure S9. The infrared absorption spectra of **2** (a) and **1** (b).

Table S1. Crystal structure and refinement details of **2** and **1**.

Compound	**2_298 K**	**2_410 K**	**1**
Formula	$C_{12}H_{18}Cl_4CuN_4$	$C_{12}H_{18}Cl_4CuN_4$	$C_{12}H_{18}Cl_4CuN_4$
Formula weight	423.64	423.64	423.64
Temperature	298 K	410 K	299 K
Crystal system	monoclinic	monoclinic	monoclinic
Space group	*C*2/*c*	*C*2/*c*	*C*2/*c*
a/Å	11.3689(18)	11.3440(9)	13.3776(3)
b/Å	12.3269(11)	12.2584(7)	8.3515(2)
c/Å	14.343(3)	14.3901(13)	15.9482(3)
α/°	90	90	90
β/°	113.26(2)	112.637(10)	93.345(2)
γ/°	90	90	90
V/Å^3	1846.7(6)	1846.9(3)	1778.75(7)
Z	4	4	4
ρ/g.cm^3	1.524	1.524	1.582
$R_1[I >= 2\sigma(I)]$	0.0563	0.0690	0.0351
$wR_2[I >= 2\sigma(I)]$	0.1462	0.2029	0.1043
GOF	1.081	1.016	1.083

Table S2. Crystal structure related bond length [Å] and bond angle [°] for **2** at 298 K.

Length (Å)			
Cu1-Cl1[1]	2.2689(12)	Cu1-Cl2	2.2640(11)
Cu1-Cl1	2.2689(12)	Cu1-Cl2[1]	2.2640(11)
N1-C1	1.359(6)	C4-C3	1.517(7)
N1-C6	1.354(5)	C5-C6	1.409(6)
N2-C6	1.351(5)	C3-C5	1.380(6)
C1-C2	1.354(7)	C3-C2	1.414(7)

Angle (°)			
Cl1-Cu1-Cl1[1]	94.61(6)	C3-C2-C1	119.9(4)
Cl2[1]-Cu1-Cl[1]	94.93(4)	C4-C3-C2	121.3(5)
Cl2[1]-Cu1-Cl1[1]	146.41(6)	C5-C3-C2	118.1(4)
Cl2-Cu1-Cl1	146.41(6)	C5-C3-C4	120.7(5)
Cl2-Cu1-Cl1[1]	94.93(4)	C6-C5-C3	121.2(4)
Cl2[1]-Cu1-Cl2	94.69(6)	N2-C6-N1	119.2(4)
C6-N1-C1	122.3(4)	C5-C6-N1	117.8(4)
C2-C1-N1	120.7(4)	C5-C6-N2	123.1(4)

Symmetric code: [1]1-X, +Y, 1/2-Z

Table S3. Crystal structure related bond length [Å] and bond angle [°] for **1** at 299 K.

Length (Å)			
Cu1-Cl1[1]	2.2511 (6)	Cu1-Cl2	2.2338 (6)
Cu1-Cl1	2.2511 (6)	Cu1-Cl2[1]	2.2338 (6)
N1-C1	1.335 (3)	C3-C2	1.358 (4)
N1-C6	1.361 (4)	C4-C6	1.358 (4)
N2-C1	1.331 (4)	C3-C4	1.398 (4)
C1-C2	1.407 (4)	C4-C5	1.500 (4)

Angle (°)			
Cl1-Cu1-Cl1[1]	143.68 (4)	Cl2-Cu1-Cl1[1]	97.53 (3)
Cl2[1]-Cu1-Cl1[1]	95.89 (3)	Cl2-Cu1-Cl1	95.89 (3)
Cl2[1]-Cu1-Cl1	97.53 (3)	Cl2[1]-Cu1-Cl2	135.99 (4)
C3-C2-C1	119.4 (2)	C4-C3-C2	122.7 (2)
C6-N1-C1	123.6 (2)	C5-C4-C6	121.8 (2)
C6-C4-C3	116.0 (2)	C2-C1-N1	117.0 (2)
C3-C4-C5	122.3 (2)	C4-C6-N1	121.3 (2)
N1-C1-N2	119.5 (2)	C2-C1-N2	123.5 (2)

Symmetric code: [1]1-X, +Y, 1/2-Z

Table S4. Hydrogen bonds for **2** at 298 K.

D–H···A	d(D–H)/Å	d(H···A)/Å	d(D···A)/Å	D–H···A/°
N1–H1···Cl1[1]	0.860	2.716	3.372(5)	134.2(4)
N1–H1···Cl2[2]	0.860	2.653	3.409(5)	147.4(4)
N2–H2b···Cl2[2]	0.860	2.46	3.410(5)	168.8(8)

Symmetric code: [1]-1/2+X, 1/2+Y, Z; [2]1/2-X, 1/2+Y, 1/2-Z

Table S5. Hydrogen bonds for **1** at 299 K.

D–H···A	d(D–H)/Å	d(H···A)/Å	d(D···A)/Å	D–H···A/°
N1–H1···Cl1	0.86	2.420(2)	3.253(2)	163.33(6)

Symmetric code: [1]1-X, +Y, 1/2-Z; [2]3/2-X, -1/2+Y, 1/2-Z; [3]3/2-X, 1/2-Y, 1-Z

Table S6. Crystal structure related bond length [Å] and bond angle [°] for **2** at 410 K.

Length (Å)			
Cu1-Cl1	2.2467(12)	C6-N2	1.328(6)
Cu1-Cl1[1]	2.2467(12)	C6-C5	1.382(7)
Cu1-Cl2	2.2441(13)	C5-C3	1.347(8)

Cu1-Cl2[1]	2.2441(13)	C3-C2	1.413(8)
N1-C6	1.343(6)	C3-C4	1.507(8)
N1-C1	1.338(7)	C1-C2	1.329(8)

Angle (°)			
Cl1[1]-Cu1-Cl1	94.96(7)	C5-C6-N1	117.5(5)
Cl2[1]-Cu1-Cl1[1]	95.36(5)	C5-C6-N2	124.3(5)
Cl2[1]-Cu1-Cl1	145.41(8)	C3-C5-C6	122.0(5)
Cl2-Cu1-Cl1[1]	145.41(8)	C2-C3-C5	117.7(5)
Cl2-Cu1-Cl1	95.36(5)	C4-C3-C5	122.1(6)
Cl2[1]-Cu1-Cl2	94.60(7)	C4-C3-C2	120.2(6)
C1-N1-C6	122.2(5)	C2-C1-N1	121.0(5)
N2-C6-N1	118.2(5)	C1-C2-C3	119.6(5)

Symmetric code: [1]2-X, +Y, 1/2-Z

Table S7. Hydrogen bonds for **2** at 410 K.

D–H···A	d(D–H)/Å	d(H···A)/Å	d(D···A)/Å	D–H···A/°
N1–H1···Cl1	0.8600	2.714(4)	3.373(4)	134.51(9)
N1–H1···Cl2	0.8600	2.633(5)	3.389(5)	147.33(10)
N2–H2a···Cl2	0.8600	2.491(5)	3.280(5)	152.83(11)

Symmetric code: [1]3/2-X, -1/2+Y, 1/2-Z; [2]-1/2+X, -1/2+Y, +Z